Study of the first excited state of the ^{4}He nucleus in halo effective field theory

Vinícius Bruno Bet Ader
Renato Higa Bira van Kolck Gautam Rupak

Physics Institute - University of São Paulo

October 14, 2025

Overview

Overview

Motivation

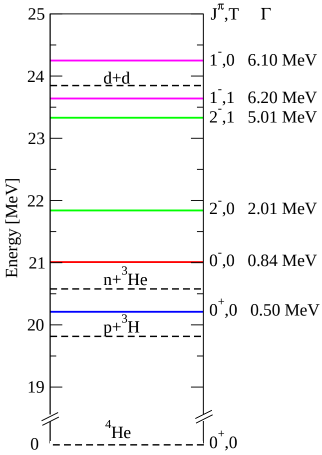

Figure 1

Motivation

- **Efimov physics:** in the unitary regime, for each three-body Efimov state, one has two corresponding four-body Efimov states, one tightly bound and the other with a halo $(3+1)$ structure (Wu et al., PRA, 2024)

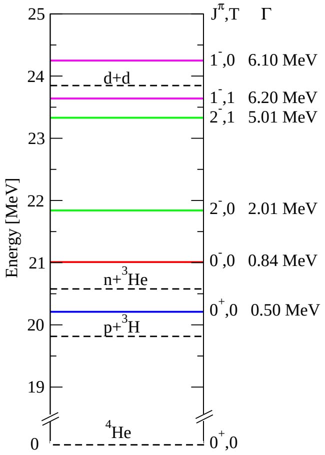

Figure 1

Motivation

- **Efimov physics:** in the unitary regime, for each three-body Efimov state, one has two corresponding four-body Efimov states, one tightly bound and the other with a halo $(3+1)$ structure (Wu et al., PRA, 2024)
- **ATOMKI anomaly:** the $p+{}^3$H and $n+{}^3$He systems play an important role in the ATOMKI anomaly description, where an excess of events in the angular distribution of the ^{3}H$(p,e^+e^-)^4$He reaction could only be explained by a possible new boson, deemed as a dark matter candidate (Krasznahorkay et al., PRC, 2021)

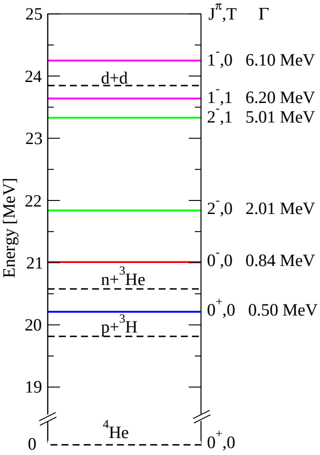

Figure 1

Overview

Partial-Wave Expansion

In two-body scattering in the centre-of-mass (CM) frame, the asymptotic behaviour of the Schrödinger equation solution for a system subjected to a spherically symmetric short-ranged interaction potential $V(r)$ is, when expanded in spherical harmonics,

$$\Phi_{\boldsymbol{k}}(\boldsymbol{r}) \approx \frac{1}{(2\pi)^3} \sum_{\ell=0}^{\infty} \frac{(2\ell+1)}{2ik} \left[[1 + 2ikf_\ell(k)] \frac{e^{ikr}}{r} - \frac{e^{-i(kr - l\pi)}}{r} \right] P_\ell(\cos\theta) \, .$$

The radial solution defines the ℓ-th element of the S-matrix

$$S_\ell(k) \equiv 1 + 2ikf_\ell(k) \, .$$

Partial-Wave Expansion

Through conservation of flux and angular momentum, which enforces unitarity, we may define

$$S_\ell(k) \equiv e^{2i\delta_\ell(k)} \quad \Rightarrow \quad T_\ell(k) \equiv \frac{2\pi}{\mu} f_\ell(k) = \frac{2\pi}{\mu} \frac{1}{k \cot \delta_\ell - ik} \,.$$

In the low-energy limit, the first term in the denominator above is analytic in k^2 and has the general expansion, valid for each angular momentum ℓ,

$$K_\ell(k^2) \equiv k^{2\ell+1} \cot \delta_\ell(k) = -\frac{1}{a_\ell} + \frac{1}{2} r_\ell k^2 + \mathcal{O}(k^4) \,,$$

known as the *effective range expansion* (*ERE*).

Charged Particles

When working with Coulomb and strong interactions, we may make use of the two-potential formalism, which states that we can separate the total amplitude as

$$T(\boldsymbol{k}', \boldsymbol{k}) = T_C(\boldsymbol{k}', \boldsymbol{k}) + T_{SC}(\boldsymbol{k}', \boldsymbol{k})\,.$$

By imposing that $\delta_\ell = \sigma_\ell + \delta'_\ell$, the partial wave decomposition becomes

$$T_C(\boldsymbol{k}', \boldsymbol{k}) = \frac{2\pi}{\mu}\sum_{\ell=0}^{\infty}(2\ell+1)\left[\frac{e^{2i\sigma_\ell}-1}{2ik}\right]P_\ell(\cos\theta)\,,$$

$$T_{SC}(\boldsymbol{k}', \boldsymbol{k}) = \frac{2\pi}{\mu}\sum_{\ell=0}^{\infty}(2\ell+1)e^{2i\sigma_\ell}\left[\frac{e^{2i\delta'_\ell}-1}{2ik}\right]P_\ell(\cos\theta)\,.$$

Charged Particles

Therefore, the S-matrix elements can be written as

$$S_\ell(k) = e^{2i(\sigma_\ell+\delta'_\ell)} = 1 + 2ik\left[f_\ell^C(k) + f_\ell^{SC}(k)\right]$$
$$= e^{2i\sigma_\ell} + i\frac{\mu k}{2\pi}\, T_\ell^{SC}(k)\,.$$

In the low-energy limit, we must define the Coulomb-modified effective range function

$$K_\ell^C(k^2) \equiv k^{2\ell+1}\frac{C_\eta^{(\ell)2}}{C_\eta^{(0)^2}}\left[2\eta H(\eta) + C_\eta^{(0)^2}(\cot\delta'_\ell - i)\right]$$
$$\approx -\frac{1}{a_\ell} + \frac{1}{2}r_\ell\, k^2 - \frac{1}{4}\mathcal{P}_\ell\, k^4 + \mathcal{O}(k^6)\,.$$

Charged Particles

Therefore, the S-wave ($\ell = 0$) Coulomb-modified strong interaction transition amplitude, is given by

$$T_0^{SC}(k) = \frac{2\pi}{\mu}\left[\frac{C_\eta^{(0)^2} e^{2i\sigma_0}}{K_0^C(k^2) - 2k_C H(\eta)}\right]$$
$$\approx \frac{2\pi}{\mu}\frac{C_\eta^{(0)^2} e^{2i\sigma_0}}{-1/a_0 + r_0 k^2/2 + \cdots - 2k_C H(\eta)},$$

where

$$C_\eta^{(0)^2} = \frac{2\pi\eta}{e^{2\pi\eta}-1}, \quad \eta(k) = \frac{Z_1 Z_2 \alpha_{\rm em}\mu}{k} \equiv \frac{k_C}{k}, \quad H(x) = \psi(ix) + \frac{1}{2ix} - \ln(ix).$$

Overview

Effective Field Theory

Effective field theories (EFTs) describe the overall behaviour of the low-energy degrees of freedom in a compatible way with the desired symmetries.

In nuclear physics, the underlying theory is QCD, whose symmetries are well-known. Instead of working with quarks and gluons, one uses hadrons instead. An effective Lagrangian has the form (Hammer et al., RMP, 2020)

$$\mathcal{L} = \sum_i g_i(M_{\text{lo}}, M_{\text{hi}}, \kappa)\, O_i(\phi_j)\,.$$

Observables are computed through expansions in Q/M_{hi} and $M_{\text{lo}}/M_{\text{hi}}$, which are dictated by a scheme known as *power counting*.

Few Nucleon Systems

Below pion production, i.e., $M_{\text{hi}} \sim m_\pi \approx 140\,\text{MeV}$, we can construct an EFT with nucleons as the only degrees of freedom. With the strong interaction symmetries, the effective Lagrangian reads as

$$\mathcal{L} = \Psi^\dagger \left(i\partial_0 + \frac{\nabla^2}{2m_N} \right) \Psi + \sigma d^\dagger \left[\left(i\partial_0 + \frac{\nabla^2}{4m_N} \right) - \xi \right] d - g \left[d^\dagger \Psi\Psi + \text{h.c.} \right] + \cdots ,$$

where d is the auxiliary dimeron field.

Few Nucleon Systems

To add physical meaning to the effective Lagrangian, we must establish a power counting by connecting the low-energy observables, related to the ERE parameters, to the EFT ones. The ERE description of the scattering amplitude is given by

$$T(k) = \frac{4\pi}{m_N} \frac{1}{-\frac{1}{a} + \frac{1}{2} r k^2 + \cdots - ik} \, .$$

Whilst from QFT the LO scattering amplitude is computed via the Feynman diagram

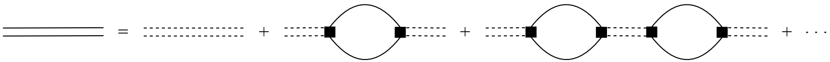

Figure 2

Few Nucleon Systems

From QFT, the scattering amplitude is proportional to the dressed interaction field (dimeron) two-point function. In leading order, it goes as

$$T^{(\mathrm{LO})}(k) = -g^2 \mathcal{D}^{(\mathrm{LO})}\left(\frac{k^2}{m_N}, \mathbf{0}\right),$$

where

$$i\mathcal{D}^{(\mathrm{LO})}(q_0, \boldsymbol{q}) = \frac{i\sigma}{-\xi - g^2 I_0(\sqrt{m_N q_0 - \boldsymbol{q}^2/4}) + i\epsilon},$$

and $I_0(k)$ is the two-body "bubble integral".

Few Nucleon Systems

To incorporate electromagnetic interactions, we perform the minimal substitution, where $\partial_\mu \to \partial_\mu + ieA_\mu$ and add to the Lagrangian the appropriate Coulombic terms. The LO amplitude, from the figure below, is given by (Higa et al., NPA, 2008)

$$T_{SC}^{(\mathrm{LO})}(k) = \frac{2\pi}{\mu}\left[\frac{C_\eta^{(0)^2} e^{2i\sigma_0}}{\sigma\frac{2\pi\xi}{\mu g^2} - i\varepsilon + \frac{2\pi}{\mu}J_0(k_C, k)}\right] \equiv \frac{2\pi}{\mu}\left[\frac{C_\eta^{(0)^2} e^{2i\sigma_0}}{\sigma\frac{2\pi\xi^{(R)}}{\mu g^2} - 2k_C H(\eta_k)}\right],$$

where, by using the *power divergence subtraction* (PDS) (Kaplan et al., PLB, 1998) scheme, we have

$$J_0(\beta, x) = \frac{\mu\beta}{\pi}\left[\frac{1}{4-D} + \ln\left(\frac{\kappa\sqrt{\pi}}{2\beta}\right) + 1 - \frac{3}{2}\gamma_E - H\left(\frac{\beta}{x}\right)\right] - \frac{\mu\kappa}{2\pi}.$$

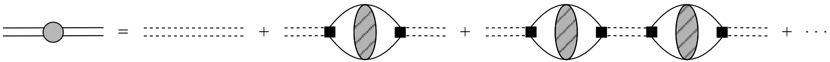

Figure 3

Overview

$p+{}^3$H and $n+{}^3$He Scattering

To study of the 0_2^+ state we consider two channels:

- Channel I: $p + {}^3$H
- Channel II: $n + {}^3$He

Therefore, we have $Q \ll m_\pi$. The breakdown scale is set by the average three-nucleon binding energy

$$M_{hi} \sim \sqrt{m_N B_{3N}} \approx 86.7\,\text{MeV}\,,$$

The low-momentum scale is set by the unnaturally small threshold difference $\Delta \approx 0.764\,\text{MeV}$, which yields

$$M_{lo} \sim Q \sim \gamma_\Delta \equiv \sqrt{2\mu_1 \Delta} \approx 32.783\,\text{MeV}\,.$$

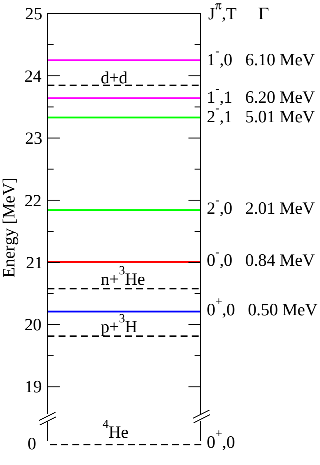

Figure 4

$p+^3$H and $n+^3$He Scattering

The free non-relativistic effective Lagrangian is written as

$$\mathcal{L}_0 = \Psi_p^\dagger\left[i\partial_0 + \frac{\nabla^2}{2m_n}\right]\Psi_p + \Psi_n^\dagger\left[i\partial_0 - (m_n - m_p) + \frac{\nabla^2}{2m_n}\right]\Psi_n$$
$$+ \Psi_t^\dagger\left[i\partial_0 + \frac{\nabla^2}{2m_h}\right]\Psi_t + \Psi_h^\dagger\left[i\partial_0 - (m_h - m_t) + \frac{\nabla^2}{2m_h}\right]\Psi_h \,.$$

Using scalar S-wave dimeron interactions, the interaction Lagrangian is (Higa et al., PRC, 2022)

$$\mathcal{L}_{int} = \sum_{\zeta,\zeta'}\chi^{(\zeta)\dagger}\left[\Xi^{(\zeta\zeta')} + \tau^{(\zeta\zeta')}\left(i\partial_0 + \frac{\nabla^2}{2M}\right)^{(\zeta\zeta')}\right]\chi^{(\zeta')}$$
$$+\sqrt{\frac{2\pi}{\mu}}\left[\chi^{(1)\dagger}\Psi_p^T\sigma_2\Psi_t + \chi^{(2)\dagger}\Psi_n^T\sigma_2\Psi_h + \mathrm{h.c.}\right].$$

$p+{}^3$H and $n+{}^3$He Scattering

As shown earlier, electromagnetism can be added straightforwardly to the Lagrangian. The Sommerfeld parameter $\eta(k)$ dictates its strength, which in turn is related to the inverse Bohr radius

$$k_C = \alpha_{\mathrm{em}} Z_p Z_t \mu_1 \approx 5.132\,\mathrm{MeV}\,.$$

However, only the first channel has both scatterers charged. To this end, the Coulomb-subtracted T-matrix is written as

$$\mathcal{T}(k) = -\frac{2\pi}{\mu}\begin{bmatrix} C_\eta^{(0)} e^{i\sigma_0} & 0 \\ 0 & 1 \end{bmatrix}\begin{bmatrix} \mathcal{D}_{11}(E,0) & \mathcal{D}_{12}(E,0) \\ \mathcal{D}_{21}(E,0) & \mathcal{D}_{22}(E,0) \end{bmatrix}\begin{bmatrix} C_\eta^{(0)} e^{i\sigma_0} & 0 \\ 0 & 1 \end{bmatrix}.$$

$p+{}^3$H and $n+{}^3$He Scattering

The propagator matrix is obtained from the following equation

$$\mathcal{D}^{-1}(E,0) = \mathcal{D}_0^{-1}(E,0) - \Sigma(E,0)\,,$$

where the free propagator matrix is given by

$$\mathcal{D}_0^{-1}(E,0) = \begin{bmatrix} \Xi^{(11)} + \tau^{(11)}E & \Xi^{(12)} + \tau^{(12)}E \\ \Xi^{(21)} + \tau^{(21)}E & \Xi^{(22)} + \tau^{(22)}E \end{bmatrix}\,.$$

and the self-energy matrix by

$$-\Sigma(E,0) = -\frac{2\pi}{\mu}\begin{bmatrix} J_0(k_C,k) & 0 \\ 0 & J_0(0,k_\star) \end{bmatrix}\,,$$

with $k_\star(k) = \sqrt{k^2 - \gamma_\Delta^2 + i0^+}$.

$p+^3$H and $n+^3$He Scattering

To rid the T-matrix of κ-dependencies, proper renormalisation group conditions are imposed, introducing ERE parameters analogues. This way, the inverse propagator matrix becomes

$$\mathcal{D}^{-1}(E,0) = \begin{bmatrix} \frac{1}{a_{11}} + 2k_C H(\eta_k) & \frac{1}{a_{12}} \\ \frac{1}{a_{12}} & \frac{1}{a_{22}} + ik_\star \end{bmatrix} - \frac{1}{2}k^2 \begin{bmatrix} r_{11} & r_{12} \\ r_{12} & r_{22} \end{bmatrix},$$

which when the inverse is taken yields

$$\mathcal{D}(E,0) = \frac{1}{G(k)} \begin{bmatrix} \frac{1}{a_{22}} - \frac{1}{2}k^2 r_{22} + ik_\star & -\frac{1}{a_{12}} + \frac{1}{2}k^2 r_{12} \\ -\frac{1}{a_{12}} + \frac{1}{2}k^2 r_{12} & \frac{1}{a_{11}} - \frac{1}{2}k^2 r_{11} + 2k_C H(\eta_k) \end{bmatrix},$$

where

$$G(k) = \left[\frac{1}{a_{11}} - \frac{1}{2}k^2 r_{11} + 2k_C H(\eta_k)\right]\left[\frac{1}{a_{22}} - \frac{1}{2}k^2 r_{22} + ik_\star\right] - \left[\frac{1}{a_{12}} - \frac{1}{2}k^2 r_{12}\right]^2.$$

$p+^3$H and $n+^3$He Scattering

Therefore, the T-matrix elements are

$$\mathcal{T}_{11}(k) = \frac{2\pi}{\mu}\frac{C_\eta^{(0)2}e^{2i\sigma_0}\left[\frac{1}{a_{22}} - \frac{1}{2}k^2 r_{22} + ik_\star\right]}{\left[\frac{1}{a_{12}} - \frac{1}{2}k^2 r_{12}\right]^2 - \left[\frac{1}{a_{11}} - \frac{1}{2}k^2 r_{11} + 2k_C H(\eta_k)\right]\left[\frac{1}{a_{22}} - \frac{1}{2}k^2 r_{22} + ik_\star\right]},$$

$$\mathcal{T}_{12}(k) = \frac{2\pi}{\mu}\frac{C_\eta^{(0)}e^{i\sigma_0}\left[-\frac{1}{a_{12}} + \frac{1}{2}k^2 r_{12}\right]}{\left[\frac{1}{a_{12}} - \frac{1}{2}k^2 r_{12}\right]^2 - \left[\frac{1}{a_{11}} - \frac{1}{2}k^2 r_{11} + 2k_C H(\eta_k)\right]\left[\frac{1}{a_{22}} - \frac{1}{2}k^2 r_{22} + ik_\star\right]},$$

$$\mathcal{T}_{22}(k) = \frac{2\pi}{\mu}\frac{\left[\frac{1}{a_{11}} - \frac{1}{2}k^2 r_{11} + 2k_C H(\eta_k)\right]}{\left[\frac{1}{a_{12}} - \frac{1}{2}k^2 r_{12}\right]^2 - \left[\frac{1}{a_{11}} - \frac{1}{2}k^2 r_{11} + 2k_C H(\eta_k)\right]\left[\frac{1}{a_{22}} - \frac{1}{2}k^2 r_{22} + ik_\star\right]}.$$

p+^{3}H and n+^{3}He Scattering

To connect our theory with the observables, the S-matrix is defined as

$$S \equiv \begin{bmatrix} e^{2i\sigma_0} + i\frac{\mu k}{\pi}\mathcal{T}_{11}(k) & i\frac{\mu\sqrt{kk_\star}}{\pi}\mathcal{T}_{12}(k) \\ i\frac{\mu\sqrt{kk_\star}}{\pi}\mathcal{T}_{21}(k) & 1 + i\frac{\mu k_\star}{\pi}\mathcal{T}_{22}(k) \end{bmatrix}.$$

In multichannel scattering, there are several ways of defining phase shifts. We're going to use the one due to Stapp, Ypsilantis and Metropolis (Stapp et al., PR, 1957)

$$S^{\mathrm{SYM}} = \begin{pmatrix} e^{2i\delta_1}\cos 2\epsilon & ie^{i(\delta_1+\delta_2)}\sin 2\epsilon \\ ie^{i(\delta_1+\delta_2)}\sin 2\epsilon & e^{2i\delta_2}\cos 2\epsilon \end{pmatrix},$$

where δ_i are the total phase shift.

Overview

Fitting Scheme

We first define the data that we will use, along with the uncertainty of the data

```
In[1]:=  Chan1Data = {{x_0^1,y_0^1},{x_1^1,y_1^1},...,{x_n^1,y_n^1}};
         Chan2Data = {{x_0^2,y_0^2},{x_1^2,y_1^2},...,{x_m^2,y_m^2}};

         FullData = Sort[Join[Chan1Data,{#1 10^6, #2} & @@@ Chan2Data]];
         Uncertainty = Table[1/(Error)^2, i, Length[FullData]];
```

If you wish to plot the data with error bars, run the following code:

```
In[2]:=  Chan1WithUncert = {#1, Around[ #2, YourUncertainty]} & @@@ Chan1Data;
         Chan2WithUncert = {#1, Around[ #2, YourUncertainty]} & @@@ Chan2Data;

         Chan1DataPlot = ListPlot[{Chan1WithUncert}];
         Chan2DataPlot = ListPlot[{Chan2WithUncert}];
```

Fitting Scheme

If your first (or any) channel function is composed of different functions, you may use

```
In[3]:=  Chan1Function[x_, cᵢ_] := Piecewise[{
             {Func1[...], x ≤ Threshold},
             {Func2[...], x > Threshold}
         }];
```

The function that will be used to fit is the following:

```
In[4]:=  CombinedFuncs[x_?NumericQ, cᵢ_?NumericQ] := Block[{result},
             Which[x < 200, result = Chan1Function[x, cᵢ];,
                 x ≥ 1000, result = Chan2Function[x/10^6, cᵢ];
             ];
             Return[result];
         ];
```

Fitting Scheme

For the curve fitting, we are going to use

```
In[5]:=  nlfSimultaneous = NonlinearModelFit[FullData, {CombinedFuncs[x, c_i]},
            {{c_1},{c_2,c_2^0},{c_3,c_3^0,c_3^inf.,c_3^sup.},...,{c_N}}, x, Weights → Uncertainty];
```

The fitted parameters can be found via

```
In[6]:=  Print[nlfSimultaneous["BestFitParameters"]];
```

while the adjusted curves are shown by running

```
In[7]:=  Chan1FittedPlot = Plot[nlfSimultaneous[x],{x,x_1^inf.,x_1^sup.}];
         Chan2FittedPlot = Plot[nlfSimultaneous[x * 10^6],{x,x_2^inf.,x_2^sup.}];
         GraphicsGrid[{{Show[Chan1DataPlot,Chan1FittedPlot],
            Show[Chan2DataPlot,Chan2FittedPlot]}}]
```

$p+^3$H and $n+^3$He Fitting

Below the second threshold, we have single-channel scattering for the first channel, whilst the second is completely closed:

$$\delta_1'(k) = -\frac{i}{2}\ln\left\{1 - \frac{2ikC_\eta^{(0)^2}\left[\frac{1}{a_{22}} - \frac{1}{2}k^2 r_{22} + ik_\star\right]}{G(k)}\right\},$$

$$\delta_2'(k) = 0\,.$$

$p+{}^3$H and $n+{}^3$He Fitting

Above the second threshold, the SYM nuclear phase shifts are given by

$$\delta_1'(k) = -\frac{i}{2}\ln\left\{\left[1 - \frac{2ikC_\eta^{(0)2}\left[\frac{1}{a_{22}} - \frac{1}{2}k^2 r_{22} + ik_\star\right]}{G(k)}\right]\sqrt{1 + \frac{4kk_\star C_\eta^{(0)2}}{f(k)}\left[\frac{1}{a_{12}^2} - \frac{1}{2}k^2 r_{12}\right]^2}\right\},$$

$$\delta_2'(k) = -\frac{i}{2}\ln\left\{\left[1 - \frac{2ik_\star\left[\frac{1}{a_{11}} - \frac{1}{2}k^2 r_{11} + 2k_C H(\eta_k)\right]}{G(k)}\right]\sqrt{1 + \frac{4kk_\star C_\eta^{(0)2}}{f(k)}\left[\frac{1}{a_{12}^2} - \frac{1}{2}k^2 r_{12}\right]^2}\right\},$$

where

$$f(k) = \left\{G(k) - 2ikC_\eta^{(0)2}\left[\frac{1}{a_{22}} - \frac{1}{2}k^2 r_{22} + ik_\star\right]\right\} \times \left\{G(k) - 2ik_\star\left[\frac{1}{a_{11}} - \frac{1}{2}k^2 r_{11} + 2k_C H(\eta_k)\right]\right\}.$$

6 parameters fit

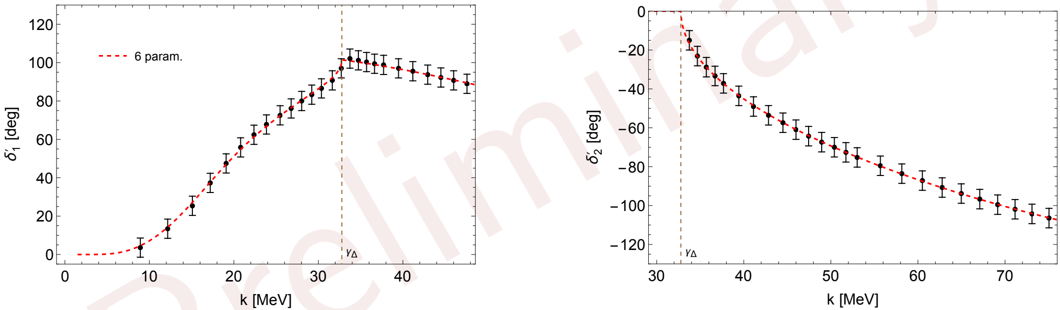

Figure 5: 6 parameters fit.

6 parameters fit

	a_{11} [fm]	a_{12} [fm]	a_{22} [fm]	r_{11} [fm]	r_{12} [fm]	r_{22} [fm]	χ^2_{red}
6 param.	17.6316	14.6473	4.91499	4.43759	-0.735538	4.91578	0.299296

Table 1: Parameter values obtained from the 6 parameters fit.

	a_{11}	a_{12}	a_{22}	r_{11}	r_{12}	r_{22}
a_{11}	1.	0.77678	0.45989	-0.96549	-0.18913	-0.69455
a_{12}	0.77678	1.	0.90042	-0.71620	-0.66858	-0.85771
a_{22}	0.45989	0.90042	1.	-0.37018	-0.71838	-0.82498
r_{11}	-0.96549	-0.71620	-0.37018	1.	0.25363	0.62622
r_{12}	-0.18913	-0.66858	-0.71838	0.25363	1.	0.48159
r_{22}	-0.69455	-0.85771	-0.82498	0.62622	0.48159	1.

Table 2: Correlation matrix for the 6 parameters fit.

5 parameters fit

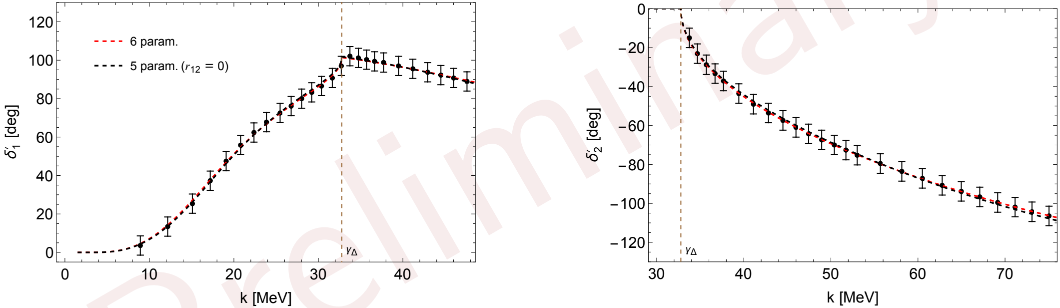

Figure 6: 6 and 5 parameters fit.

5 parameters fit

	a_{11} [fm]	a_{12} [fm]	a_{22} [fm]	r_{11} [fm]	r_{12} [fm]	r_{22} [fm]	χ^2_{red}
6 param.	17.6316	14.6473	4.91499	4.43759	-0.735538	4.91578	0.299296
5 param.	17.0013	12.5768	4.68341	4.6593	0	5.07597	0.59096

Table 3: Parameter values obtained from the 6 and 5 parameters fits.

	a_{11}	a_{12}	a_{22}	r_{11}	r_{22}
a_{11}	1.	0.90816	0.48354	-0.96945	-0.62379
a_{12}	0.90816	1.	0.79579	-0.79377	-0.79834
a_{22}	0.48354	0.79579	1.	-0.30233	-0.84921
r_{11}	-0.96945	-0.79377	-0.30233	1.	0.49932
r_{22}	-0.62379	-0.79834	-0.84921	0.49932	1.

Table 4: Correlation matrix for the 5 parameters fit.

5 parameters fit

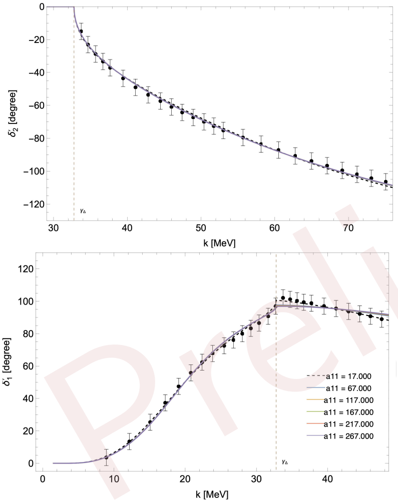

Figure 7: 6 and 5 parameters fits and residues.

Plot	a_{11}	a_{12}	a_{22}	r_{11}	r_{12}	r_{22}	$\chi^2_{\text{red.}}$
	17.00	12.58	4.68	4.66	0	5.08	–
	67.00	16.24	4.88	3.08	0	4.79	0.83
	117.00	17.01	4.91	2.84	0	4.75	0.90
	167.00	17.35	4.92	2.74	0	4.73	0.93
	217.00	17.53	4.93	2.69	0	4.72	0.95
	267.00	17.65	4.93	2.66	0	4.72	0.96

Table 5

- a_{11} enters as a higher order correction!

4 parameters fit

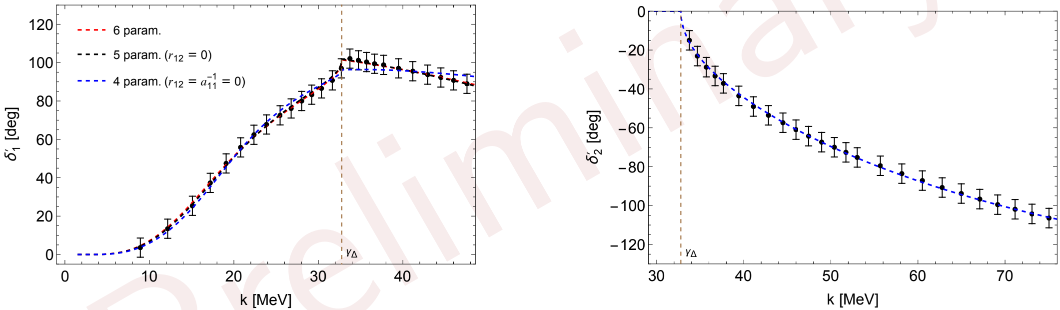

Figure 8: 6,5 and 4 parameters fit.

4 parameters fit

	a_{11} [fm]	a_{12} [fm]	a_{22} [fm]	r_{11} [fm]	r_{12} [fm]	r_{22} [fm]	χ^2_{red}
6 param.	17.6316	14.6473	4.91499	4.43759	-0.735538	4.91578	0.299296
5 param.	17.0013	12.5768	4.68341	4.6593	0	5.07597	0.59096
4 param.	10^{10}	18.1906	4.95336	2.51666	0	4.69215	1.01797

Table 6: Parameter values obtained from the 6, 5 and 4 parameters fits.

	a_{12}	a_{22}	r_{11}	r_{22}
a_{12}	1.	0.960538	0.762616	-0.758696
a_{22}	0.960538	1.	0.664053	-0.846256
r_{11}	0.762616	0.664053	1.	-0.517207
r_{22}	-0.758696	-0.846256	-0.517207	1.

Table 7: Correlation matrix for the 4 parameters fit.

Overview

1. Motivation
2. Quantum Scattering Theory
3. Effective Field Theory
4. $p+{}^3$H and $n+{}^3$He Scattering
5. Simultaneous Fitting
6. Final Remarks
   - Conclusion
   - Future Prospects

Conclusion

- The theory is capable of describing the data with all it's details;

Conclusion

- The theory is capable of describing the data with all it's details;
- Considering both scattering lengths and effective ranges, there is a clear overparameterisation of the theory;

Conclusion

- The theory is capable of describing the data with all it's details;
- Considering both scattering lengths and effective ranges, there is a clear overparameterisation of the theory;
- A systematic reduction on the number of parameters leads to a better understanding of the theory's power counting.

Future Prospects

- One might study the evolution of the 0_2^+ resonance to a bound Efimov descendant as one artificially turns off the isospin-breaking terms;

Future Prospects

- One might study the evolution of the 0_2^+ resonance to a bound Efimov descendant as one artificially turns off the isospin-breaking terms;
- We intend to calculate the radiative capture of the reactions $^3\mathrm{H}(p,\gamma)^4\mathrm{He}^*$ and $^3\mathrm{He}(n,\gamma)^4\mathrm{He}^*$, as it may shed light on the ATOMKI anomaly.

Thank you!

Residues

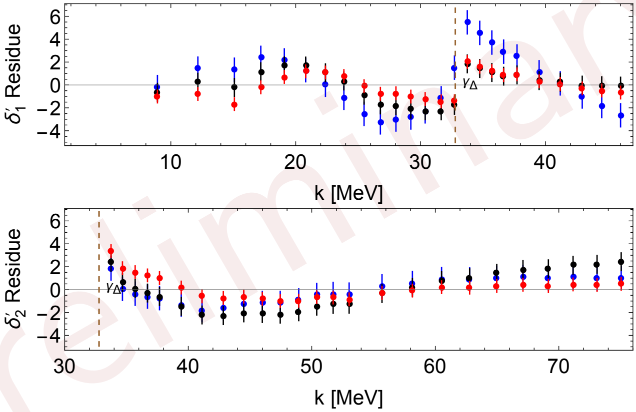

Figure 9: 6, 5 and 4 parameters fits and residues in red, black and blue respectively.

3 parameters fit (with a)

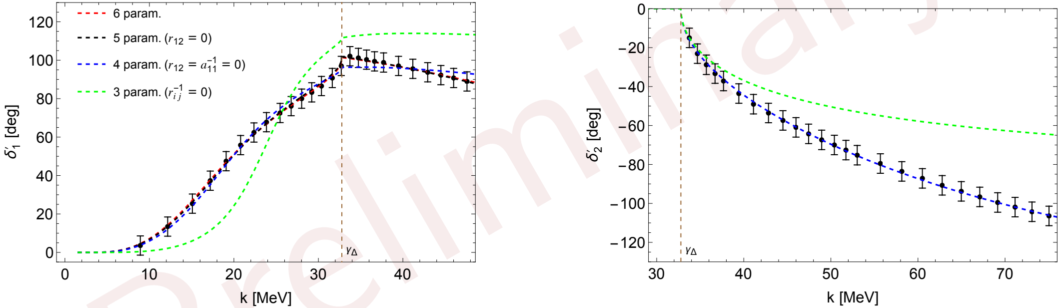

Figure 10: 6, 5, 4 and 3 parameters fit.

3 parameters fit (with a)

Preliminary

	a_{11} [fm]	a_{12} [fm]	a_{22} [fm]	r_{11} [fm]	r_{12} [fm]	r_{22} [fm]	$\chi^2_{\text{red.}}$
6 param.	12.544	11.158	4.54173	4.9517	-0.475504	4.70458	0.1327
5 param.	11.9718	10.2827	4.41197	5.21726	0	4.83437	0.2721
4 param.	∞	16.4758	4.77115	2.37467	0	4.29	0.97711
3 param.	7.20×10^8	14.2843	5.95597	0	0	0	115.109

Table 8: Parameter values obtained from the 6, 5, 4 and 3 parameters fits.

	a_{11}	a_{12}	a_{22}
a_{11}	1.	-0.999808	-0.915999
a_{12}	-0.999808	1.	0.907956
a_{22}	-0.915999	0.907956	1.

Table 9: Correlation matrix for the 3 parameters fit (using a_{ij}).

3 parameters fit (with $\alpha = a^{-1}$)

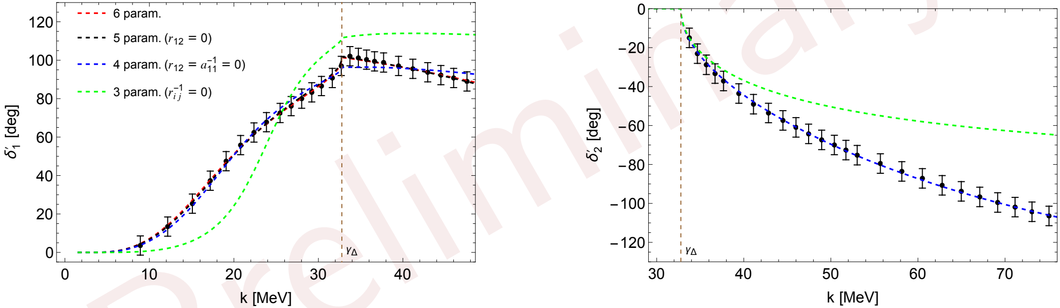

Figure 11: 6,5,4 and 3 parameters fit.

3 parameters fit (with $\alpha = a^{-1}$)

	a_{11} [fm]	a_{12} [fm]	a_{22} [fm]	r_{11} [fm]	r_{12} [fm]	r_{22} [fm]	$\chi^2_{\text{red.}}$
6 param.	12.544	11.158	4.54173	4.9517	-0.475504	4.70458	0.1327
5 param.	11.9718	10.2827	4.41197	5.21726	0	4.83437	0.2721
4 param.	∞	16.4758	4.77115	2.37467	0	4.29	0.97711
3 param.	-14.053	-2.27 $\times 10^{9}$	13.032	0	0	0	33.477

Table 10: Parameter values obtained from the 6, 5, 4 and 3 parameters fits.

	α_{11}	α_{12}	α_{22}
α_{11}	1.	0.254501	-2.05 $\times 10^{-9}$
α_{12}	0.254501	1.	-5.23959 $\times 10^{-10}$
α_{22}	-2.05 $\times 10^{-9}$	-5.23959 $\times 10^{-10}$	1.

Table 11: Correlation matrix for the 3 parameters fit (using α_{ij}).